Triple Eyewall in Hurricane Juliette

BY BRIAN D. MCNOLDY

Hurricane eyewalls are one of the more enigmatic phenomena in the atmosphere. Even more mysterious are concentric eyewall cycles: the development of a ring of deep convection within a larger ring of deep convection, with a "moat" between them. On radar, the moat would appear as a nearly echo-free annulus, while an eyewall would appear as an annulus with radar echoes typically greater than 35 dB*Z*. From the first days of aircraft reconnaissance into hurricanes during the 1940s, these "double eyes" were occasionally observed in strong storms, and the advent of satellite meteorology in the 1960s has provided additional cases that we otherwise would not have known about. In particular, passive microwave imagery is the most ideal and prominent tool available for monitoring the internal precipitation structure, concentric eyewalls, and eyewall replacement cycles (Hawkins and Helveston 2004).

Concentric eyewalls are ephemeral; once formed, they typically are not maintained for much longer than 12 h. As the new outer eyewall forms, the original inner eyewall usually lacks the necessary inflow to maintain itself, and it gradually dissipates. In time, dynamic processes cause the outer eyewall to contract, and the process can repeat itself; this is called an eyewall replacement cycle (Black and Willoughby 1992). Multiple eyewalls are more commonly observed in intense tropical cyclones (i.e., Category 3, 4, and 5 on the Saffir–Simpson scale; Simpson 1974). From a study of western North Pacific tropical cyclones (TCs) during 1969–71, Willoughby et al. (1982) estimated that approximately 53% of intense TCs (winds greater than 65 m s^{-1}) exhibit concentric eyewalls, while only 14% of weaker TCs do.

AFFILIATIONS: MCNOLDY—Department of Atmospheric Science, Colorado State University, Fort Collins, Colorado
CORRESPONDING AUTHOR: Brian D. McNoldy, Colorado State University, Fort Collins, Colorado 80523-1371
E-mail: mcnoldy@atmos.colostate.edu
DOI: 10.1175/BAMS-85-11-1663

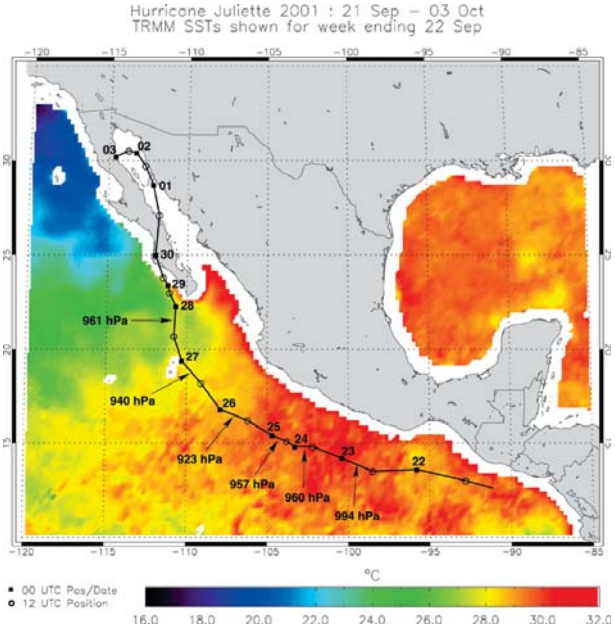

FIG. 1. Best-track positions of Juliette provided by the NOAA National Hurricane Center. The 0000 UTC positions are denoted by a solid square, and the 1200 UTC positions are denoted by an open circle; the date is marked at the top or right of each 0000 UTC square. The track is plotted over weekly mean sea surface temperature contours, which are valid in the week from 15 to 22 Sep 2001 (i.e., the prestorm period). One week later, the SSTs cooled by 6°–8°C in the wake of Juliette after the hurricane had passed over the area at its peak intensity on 24–27 Sep (not shown). TRMM data are produced by Remote Sensing Systems and sponsored by NASA's Earth Science Information Partnerships and NASA's TRMM Science Team.

An interesting example of multiple eyewalls occurred during September 2001 in the eastern North Pacific basin. Tropical Depression 11 formed off the Guatemalan coast at 0600 UTC on 21 September and moved west-northwest, generally following the coastline. At 1200 UTC on 21 September, it was upgraded to Tropical Storm Juliette; then, at 1200 UTC on 23 September, it was upgraded to Hurricane Juliette. Two days after formation and slow organization, explosive deepening occurred toward the end of 23 Sep-

tember. The central pressure fell 35 hPa in the 12-h period ending at 0000 UTC on 24 September (2.9 hPa hr^{-1}). Juliette reached a central minimum sea level pressure (intensity) of 941 hPa, then weakened slightly over the next day. Twenty-four hours later (1800 UTC on 25 September), the storm reintensified to a peak intensity of 923 hPa and 64 m s^{-1}. Figure 1 shows the track, selected intensities along the track, and weekly mean sea surface temperatures in the region (all times, pressures, and positions given are

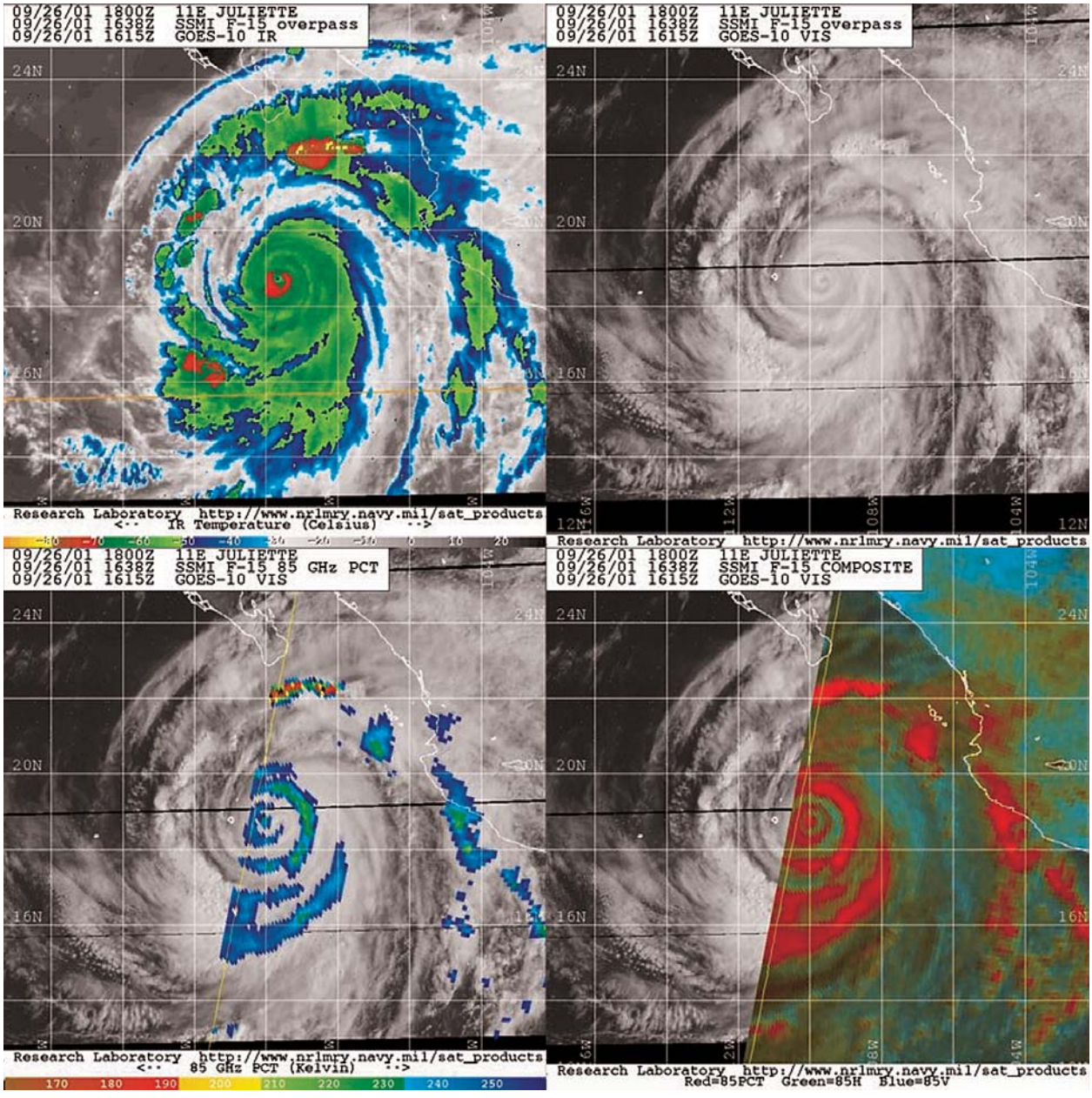

FIG. 2. Hurricane Juliette on 26 Sep 2001 at 1638 UTC. (Upper left) *GOES-10* infrared (10.7-μm) image showing cloud-top temperatures; (upper right) *GOES-10* visible image that shows a very tightly-wound inner core; (lower left) SSM/I 85-GHz polarization-corrected temperature (PCT) image, depicting areas of heaviest precipitation; and (lower right) SSM/I 85-GHz composite microwave imagery showing upper-level heavy precipitation (red) and low-level clouds and moisture bands (green). Note that in the latter two panels, *GOES-10* data are used outside the SSM/I swath. See Hawkins et al. (2001) for a detailed explanation of these products. Image courtesy of the Naval Research Laboratory in Monterey, California.

from the NOAA National Hurricane Center Best Track dataset).

Beginning at approximately this time, a second eyewall formed outside the inner ring around the "pinhole" eye. By 26 September, aircraft reconnaissance data and satellite microwave imagery indicated that a third eyewall had formed outside the inner two eyewalls. The Special Sensor Microwave Imager (SSM/I) 85-GHz channel is able to display the precipitation structure of the TC, even when other imagery is obscured by a cirrus shield (see Hawkins et al. 2001 and Spencer et al. 1989 for details on the remote-sensing aspects). Figure 2 shows an overpass on 26 September at 1638 UTC that just caught the inner core on the edge of a swath. From this image, it appears that there are three concentric eyewalls, with a moat-like feature between each of them. *GOES-10* infrared and visible imagery is displayed in the top two panels, but at these frequencies, only the top cirrus shield can be seen. The lower-right panel of this figure clearly shows the inner two complete eyewalls; unfortunately, the swath missed about one-third of the outer eyewall, so it is difficult to conclude that it was a complete ring. However, a reconnaissance aircraft did provide independent confirmation; it happened to be flying in the storm just one hour after the SSM/I overpass.

On 25 and 26 September, a U.S. Air Force Reserve Command WC-130 "Hurricane Hunter" aircraft from the 53rd Weather Reconnaissance Squadron flew through the intense hurricane and not only found the second-lowest pressure ever measured in the eastern North Pacific (923 hPa), but also a very unique inner-core configuration. On 25 September, the aircraft was in the storm from 1745 to 2037 UTC, and on 26 September it was in the storm from 1653 to 1933 UTC. The highlight of the flights was on 26 September, when the crew found three concentric eyewalls, defined by three peaks in tangential wind in each of the radial legs and by three complete rings of enhanced radar reflectivity (e.g., Willoughby et al. 1982), with radii of 11, 56, and 90 km. This matches the eyewall diameter estimates one can make using the microwave imagery in the lower two panels of Fig. 2. Data from the Hurricane Hunter aircraft are shown in Fig. 3. The data shown were taken from 3 km altitude with 30-s temporal resolution (5.5-km radial resolution). The top panel shows the tangential winds from radial legs in the northwest quadrant of the storm on 25 and 26 September, and the bottom panel shows the relative vorticity from that same quadrant on both days. Some of the data in other quadrants

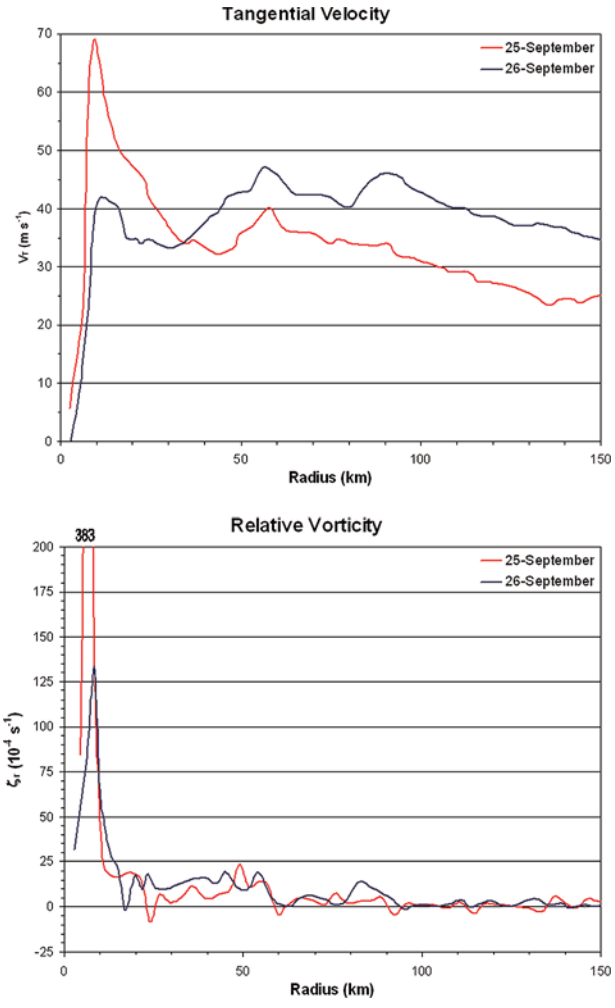

FIG. 3. Radial profiles of (top) tangential velocity and (bottom) relative vorticity through the northwest quadrant of Juliette on 25 and 26 Sep at 1819–1849 and 1722–1755 UTC, respectively. The northwest quadrant is representative of the other three but was chosen for its higher resolution and better quality data on both days. The relevant features are the two peaks in tangential velocity on 25 Sep at 9 and 58 km (with corresponding peaks in relative vorticity at 7 and 55 km) and the three peaks in tangential velocity on 26 Sep at 11, 56, and 90 km (with corresponding peaks in relative vorticity at 9, 54, and 82 km).

were noisier or of poorer resolution, so this quadrant alone was chosen for containing the best data available; however, the features shown are azimuthally consistent. In this simplified radial perspective, the relative vorticity is generated solely by the radial gradient of the tangential wind; the steepness of the vorticity curves may play a role in the formation of moats. From the figure, one can see that the innermost

eyewall produced the sharpest drop-off in vorticity, and the second (and third) eyewalls produced peaks in vorticity that are not as dramatic, but still above the noise of minor fluctuations.

So why do moats form? The answer is unclear, but it is believed that both the 3-D coupled thermodynamics/dynamics as well as 2-D vorticity dynamics play critical roles. Rozoff et al. (2004) show a significant dewpoint depression of 8°–10°C in the moat between concentric eyewalls in Hurricane Gilbert in 1988, indicating subsidence, which inhibits convection. However, the focus of their paper is on a difference in relative magnitude between vorticity and deformation as being another mechanism responsible for moat formation. Rotation-dominated regions, which are found inside the radius of maximum wind and further outside of steep negative vorticity gradients, allow coherent structures such as clouds and mesovortices to exist (see Kossin et al. 2002 for a collection of hurricane mesovortex observations, and references therein). Strain-dominated regions, found just outside the radius of maximum wind in the steep negative vorticity gradient, are basically filled with vorticity filaments and cloud debris. In fact, one could consider a "filamentation time scale" for strain-dominated regions. If deformation is sufficiently greater than vorticity, then the filamentation time scale (defined as a temporal measure of the relative difference between deformation and vorticity) is shorter than the convective time scale (defined to be the approximate time required to develop a thunderstorm in the Tropics—about 30 min.), and no deep cloud can form. The greater the difference in magnitudes, the shorter the filamentation time scale. Conversely, if the filamentation time scale is longer than the convective time scale, deep clouds have time to form and possibly organize into spiral bands or another eyewall.

This conveniently leads to the case of double—or even triple—eyewalls. Once the initial eyewall forms and perhaps establishes a moat, deep convection is free to organize outside of the moat. This convection can be axisymmetrized (ignoring external influences such as vertical wind shear), and a new ring of deep convection (i.e., a concentric eyewall) is born. Sometimes in just a few hours the new outer eyewall will dominate, the inner eyewall dissipates, and an eyewall replacement cycle is completed. Further research is needed on this topic, investigating the 3-D structure of filamentation times and the relative role of subsidence.

FOR FURTHER READING

Black, M. L., and H. E. Willoughby, 1992: The concentric eyewall cycle of Hurricane Gilbert. *Mon. Wea. Rev.*, **120**, 947–957.

Hawkins, J. D., and M. Helveston, 2004: Tropical cyclone multiple eyewall characteristics. Preprints, *26th Conf. on Hurricanes and Tropical Meteorology*, Miami Beach, FL, Amer. Met. Soc., 276–277.

——, T. F. Lee, J. Turk, C. Sampson, J. Kent, and K. Richardson, 2001: Real–time internet distribution of satellite products for tropical cyclone reconnaissance. *Bull. Amer. Met. Soc.*, **82**, 567–578.

Kossin, J. P., B. D. McNoldy, and W. H. Schubert, 2002: Vortical swirls in hurricane eye clouds. *Mon. Wea. Rev.*, **130**, 3144–3149.

Rozoff, C. M., W. H. Schubert, B. D. McNoldy, and J. P. Kossin, 2004: Rapid filamentation zones in intense tropical cyclones. *J. Atmos. Sci.*, in press.

Simpson, R. H., 1974: The hurricane disaster potential scale. *Weatherwise*, **27**, 169–186.

Spencer, R. W., H. M. Goodman, and R. E. Hood, 1989: Precipitation retrieval over land and ocean with the SSM/I: Identification and characteristics of the scattering signal. *J. Atmos. Oceanic Technol.*, **6**, 254–273.

Willoughby, H. E., J. A. Clos, and M. G. Shoreibah, 1982: Concentric eyewalls, secondary wind maxima, and the evolution of the hurricane vortex. *J. Atmos. Sci.*, **39**, 395–411.